Supplementary Material (SM) for:

A detailed particle model for polydisperse aggregate particles

Casper S. Lindberg[a,c], Manoel Y. Manuputty[a,c], Edward K. Y. Yapp[b,c], Jethro Akroyd[a,c], Rong Xu[b,c], Markus Kraft[a,b,c,*]

[a] *Department of Chemical Engineering and Biotechnology, University of Cambridge, Philippa Fawcett Drive, Cambridge, CB3 0AS, United Kingdom*
[b] *School of Chemical and Biomedical Engineering, Nanyang Technological University, 62 Nanyang Drive, 6357459, Singapore*
[c] *Cambridge Centre for Advanced Research and Education in Singapore (CARES), CREATE Tower, 1 Create Way, 138602, Singapore*

---

1. Ballistic cluster cluster aggregation

1.1. Free-molecular collisions

A simple test case was created to determine the average fractal dimension generated by the BCCA algorithm. A zero-dimensional batch reactor was simulated with an initial population of 4 096 monodisperse spherical particles with diameter $d_\mathrm{p} = 1.81$ nm. Particles were allowed to coagulate in the free-molecular regime with no other processes turned on. The simulation was repeated 8 times producing a total of 25 794 particles with a median of 118 primaries per particle.

The fractal dimension D_f and pre-factor k_f were estimated by fitting the standard fractal relationship to the data, expressed in the following form:

$$\ln\left(\frac{d_\mathrm{g}}{d_\mathrm{p,avg}}\right) = \frac{1}{D_\mathrm{f}}\ln(n_\mathrm{p}) - \frac{1}{D_\mathrm{f}}\ln(k_\mathrm{f}). \tag{1}$$

The diameter of gyration d_g is calculated as per Jullien [1]:

$$d_\mathrm{g}^2 = \frac{2}{n_\mathrm{p}^2}\sum_{i,j}\left(\mathbf{x}_i - \mathbf{x}_j\right)^2, \tag{2}$$

which assumes that the primary mass is concentrated at the primary centre. The data and a least squares fit to a subset of the data – particles with $n_\mathrm{p} \geq 16$ – are shown in Fig. 1(a). Figure 1(b) shows how the fitted values of D_f and k_f vary as function of the minimum number of primaries per aggregate $n_\mathrm{p,min}$ included in the fit. Both D_f and k_f show slight sensitivity to small values of $n_\mathrm{p,min}$ and converge for $n_\mathrm{p,min} > 10$.

*Corresponding author
Email address: mk306@cam.ac.uk (Markus Kraft)

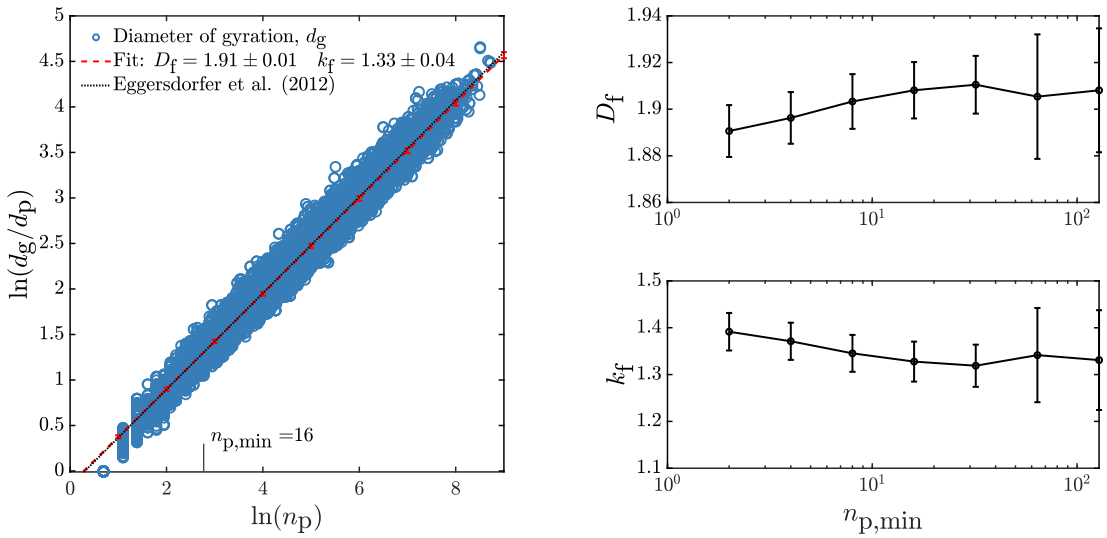

Figure S1: BCCA with particle selection based on the free-molecular kernel. (a): estimate of fractal dimension and prefactor by least squares fit to aggregates with $n_p \geq 16$; the result reported by Eggersdorfer and Pratsinis [2] is included for reference; error bars indicate the confidence interval with $P = 0.999$. (b): fractal dimension and prefactor as a function of $n_{p,min}$ with $P = 0.999$ confidence intervals. The error bars increase with increasing $n_{p,min}$ due to the smaller sample size.

This behaviour is expected since particles are not fractal-like in the small n_p limit. The values obtained in Fig. 1(a) ($D_f = 1.91 \pm 0.01$ and $k_f = 1.33 \pm 0.04$) are in good agreement with the results reported by Eggersdorfer and Pratsinis [2] ($D_f = 1.89 \pm 0.03$ and $k_f = 1.36 \pm 0.10$) and Jullien [1] ($D_f = 1.91 \pm 0.03$, k_f not reported).

1.2. Uniform particle selection

A second test case was created in which particles are uniformly selected for collision from the particle ensemble. The test case was initialised with a population of 4 096 monodisperse spherical particles with diameter $d_p = 1.81$ nm. The simulation was repeated 8 times producing a total of 16 667 particles with a median of 172 primaries per particle.

The data and a least squares fit to a subset of the data with $n_p \geq 16$ are shown in Fig. 2(a). Figure 2(b) shows how the fitted values of D_f and k_f vary as function of the minimum number of primaries per aggregate $n_{p,min}$. Both D_f and k_f display similar behaviour with respect to $n_{p,min}$ as the free-molecular case.

The fractal dimension D_f obtained in Fig. 2(a) ($D_f = 1.91 \pm 0.01$) is in good agreement with the value obtained by free-molecular collisions and the values reported by Jullien [1] and Eggersdorfer and Pratsinis [2]. The fractal prefactor, on the other hand, appears to be sensitive to the method of particle selection.

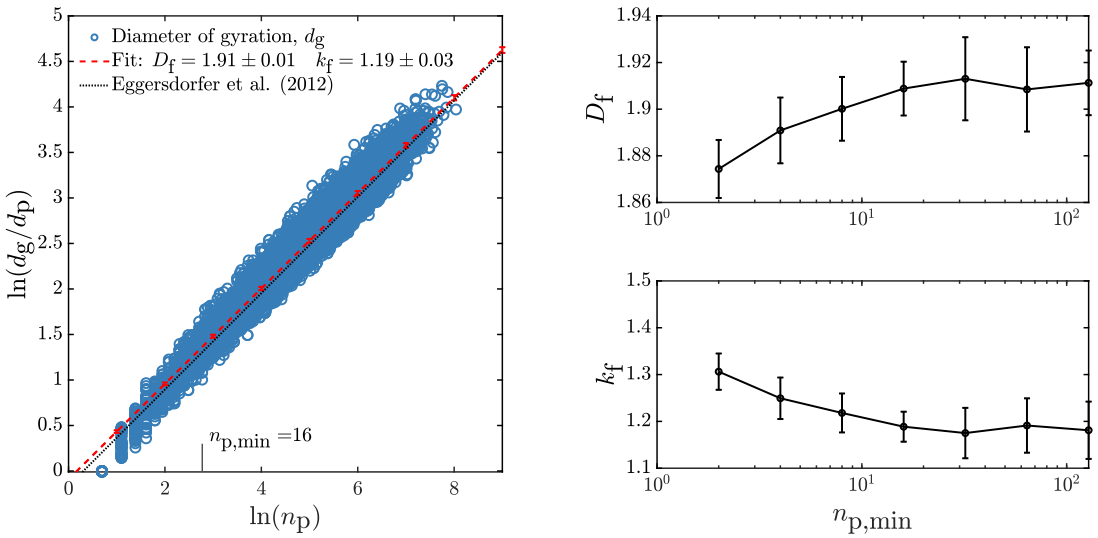

Figure S2: BCCA with uniform selection of particles for collision. (a): estimate of fractal dimension and prefactor by least squares fit to aggregates with $n_p \geq 16$; the result reported by Eggersdorfer and Pratsinis [2] is included for reference; error bars indicate the confidence interval with $P = 0.999$. (b): fractal dimension and prefactor as a function of $n_{p,min}$ with $P = 0.999$ confidence intervals. The error bars increase with increasing $n_{p,min}$ due to the smaller sample size.

Uniform selection yields a lower fractal prefactor ($k_f = 1.19 \pm 0.03$) than that obtained by selection based on the free-molecular kernel – which favours collisions between small and large particles.

2. Surface growth

Test cases are presented for the surface growth sub-model of the detailed particle model. The first, constant growth model, evaluates the particle transformation model against two limiting cases. In the next two cases, the behaviour of the detailed particle model under collision limited and surface area dependent growth is compared to one- and two-dimensional particle models with different model assumptions.

2.1. Constant growth

The aim of this test case is to test the particle transformation model for surface growth. For this test the actual growth rate is arbitrary; thus, for the sake of simplicity, a constant rate of growth β is assumed:

$$\frac{\mathrm{d}V}{\mathrm{d}t} = \beta. \tag{3}$$

The detailed particle model is evaluated against the analytical solutions for two limiting cases: growth of a single sphere with the same initial volume, and growth of the same initial number of spherical primary particles that remain in point contact. The model equations for the two limiting cases are given below.

2.1.1. Model equations

Spherical primaries in point contact. $n_{\mathrm{p},0}$ primaries of radius $r_{\mathrm{p},0}$ are assumed to remain in point contact during growth. The initial aggregate volume and surface area are

$$V_0 = \frac{4}{3}\pi r_{\mathrm{p},0}^3 n_{\mathrm{p},0}, \tag{4}$$

$$S_0 = 4\pi r_{\mathrm{p},0}^2 n_{\mathrm{p},0}. \tag{5}$$

Integrating Eq (3): the time evolution of the particle volume is

$$V(t) = \beta t + V_0, \tag{6}$$

and the surface area and primary radius evolve as

$$S(t) = 4\pi n_{\mathrm{p},0} \left(\frac{3}{4\pi n_{\mathrm{p},0}} \left(\beta t + V_0\right) \right)^{2/3}, \tag{7}$$

$$r_{\mathrm{p}}(t) = \left(\frac{3}{4\pi n_{\mathrm{p},0}} \left(\beta t + V_0\right) \right)^{1/3}. \tag{8}$$

Single sphere. The time evolution of the surface area and radius of a single sphere are:

$$S(t) = 4\pi \left(\frac{3}{4\pi} \left(\beta t + V_0\right) \right)^{2/3}, \tag{9}$$

$$r(t) = \left(\frac{3}{4\pi} \left(\beta t + V_0\right) \right)^{1/3}. \tag{10}$$

2.1.2. Results

The test case was initialised with 64 primary particles of radius $r_{\mathrm{p},0} = 0.91$ nm in point contact. In the case of the single sphere model, the initial mass is the same. For the new detailed particle model, 10 initial configurations were generated using the ballistic cluster cluster aggregation (BCCA) algorithm. Simulations were repeated twice.

Figure S3 shows the evolution of the surface area and average primary diameter against dimensionless time. The dimensionless time is defined as

$$\frac{t}{\tau} = \frac{\beta t}{V_0}. \tag{11}$$

The point contact model is a limiting case showing the fastest surface area growth and slowest growth in average primary diameter. The single sphere model with the same initial mass is the limiting case of complete rounding, in the long time limit. The detailed model starts in point contact and tends towards the single sphere due to rounding, as expected.

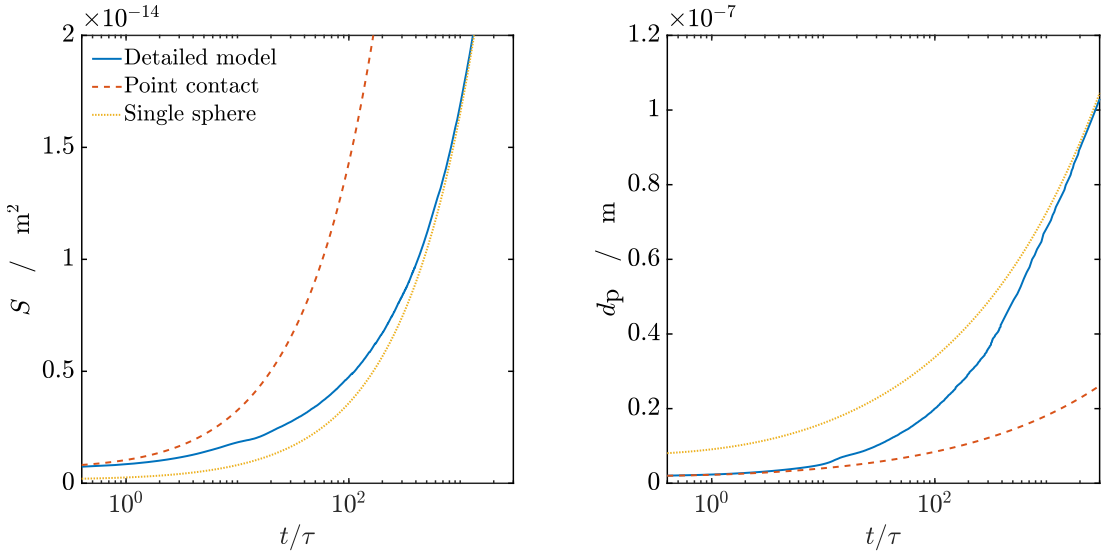

(a) Surface area

(b) Average primary diameter

Figure S3: Particle evolution with constant a constant growth rate. The detailed particle model is compared two limiting cases: growth of a single sphere, and growth of primaries that remain in point contact.

2.2. Collision limited growth

Assuming a collision limited condensation-like growth process in the free-molecular regime the growth rate is

$$\frac{\mathrm{d}V}{\mathrm{d}t} = \beta r_\mathrm{c}^2, \tag{12}$$

for some constant β and where r_c is the collision diameter.

2.2.1. Model equations

The detailed particle model is compared to three models: a spherical particle model, and a surface-volume model with and without particle rounding. The latter case corresponds to $n_{\mathrm{p},0}$ primary particles in constant point contact. The model equations are given below.

Primaries in point contact. The initial volume and surface area are given by Eqs. 4 and 5, and the collision radius [3] is

$$r_\mathrm{c} = r_\mathrm{p} n_\mathrm{p}^{1/D_\mathrm{f}}. \tag{13}$$

Equation 12 is integrated to give the time evolution of the primary diameter

$$r_\mathrm{p} = r_{\mathrm{p},0} + \frac{\beta}{4\pi} n_\mathrm{p}^{2/D_\mathrm{f}-1} t, \tag{14}$$

from which the other quantities can be derived.

Surface-volume model with rounding. A two-dimensional surface-volume model is considered. The average primary radius and number of primaries are

$$r_\mathrm{p} = \frac{3V}{S}, \tag{15}$$

$$n_\mathrm{p} = \frac{S^3}{36\pi V^2}, \tag{16}$$

and the collision radius is given by Eq. 13, which is expressed in terms of the surface area and volume:

$$r_\mathrm{c} = \frac{3V}{S}\left(\frac{S^3}{36\pi V^2}\right)^{1/D_\mathrm{f}}. \tag{17}$$

Rounding is treated as per Patterson and Kraft [4]:

$$\frac{\mathrm{d}S}{\mathrm{d}V} = 4\left(\frac{\pi}{S}\right)^{1/2}. \tag{18}$$

Finally, the model equations for the particle volume and surface area can be expressed as

$$\frac{\mathrm{d}V}{\mathrm{d}t} = \beta\left(\frac{3V}{S}\left(\frac{S^3}{36\pi V^2}\right)^{1/D_\mathrm{f}}\right)^2, \tag{19}$$

$$\frac{\mathrm{d}S}{\mathrm{d}t} = \frac{\mathrm{d}S}{\mathrm{d}V}\frac{\mathrm{d}V}{\mathrm{d}t}, \tag{20}$$

$$= 4\beta\left(\frac{\pi}{S}\right)^{1/2}\left(\frac{3V}{S}\left(\frac{S^3}{36\pi V^2}\right)^{1/D_\mathrm{f}}\right)^2. \tag{21}$$

Single sphere. A spherical particle with collision radius equal to the spherical radius grows as

$$r = r_0 + \frac{\beta}{4\pi} t, \tag{22}$$

where r_0 is the initial radius of the spherical particle.

2.2.2. Results

The model test case was initialised with 64 primary particles of radius $r_{\mathrm{p},0} = 0.91$ nm in point contact. The point contact and surface-volume models assume a constant fractal dimension of $D_{\mathrm{f}} = 1.9$, consistent with initial fractal dimension of the BCCA generated particles. In the case of the single sphere model, two different initial conditions were considered: equivalent initial mass

$$r_0 = r_{\mathrm{p},0} n_{\mathrm{p},0}^{1/3}, \tag{23}$$

and equivalent initial surface area

$$r_0 = r_{\mathrm{p},0} n_{\mathrm{p},0}^{1/2}. \tag{24}$$

For the detailed particle model, 20 initial configurations were generated using the BCCA algorithm. Simulations were repeated twice. The surface-volume model equations (Eqs. 19 and 21) were numerically integrated.

Figure S4 shows the evolution of the (aggregate) particle volume, surface area, collision diameter and average primary diameter as a function of dimensionless time for the test case. The dimensionless time is defined as

$$\frac{t}{\tau} = \frac{\beta t}{4\pi r_{\mathrm{p},0}}. \tag{25}$$

The point contact model grows much faster than the other models due to the rapid increase in collision diameter – a consequence of no rounding. For large t the surface-volume and detailed particle models converge on the spherical model due to particle rounding, as is expected. The detailed particle model converges from below as a result of slower growth in the modelled collision diameter (proportional to the gyration diameter). This is a consequence of maintaining a rigid structure while adding mass uniformly to the surface of the particle.

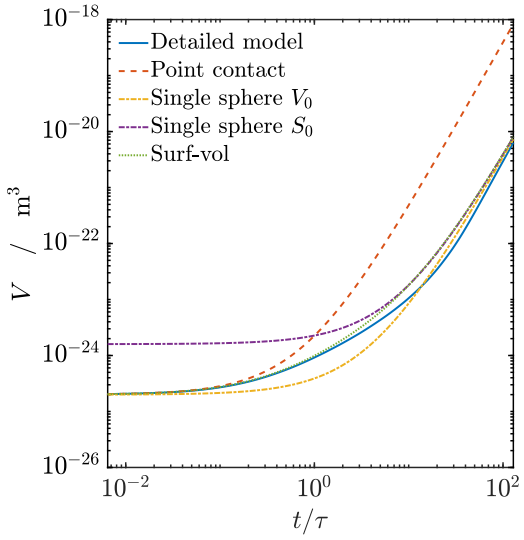

(a) Volume

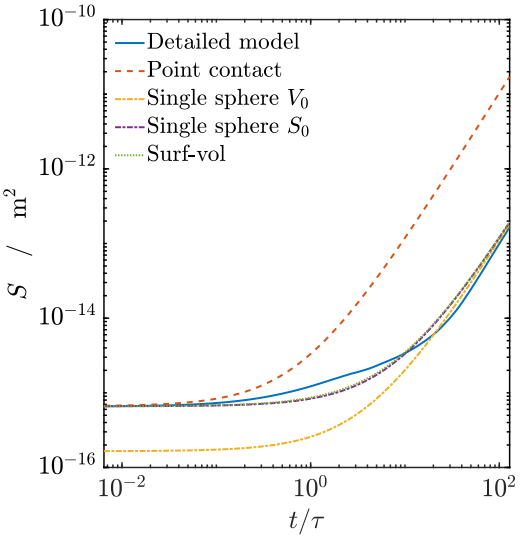

(b) Surface area

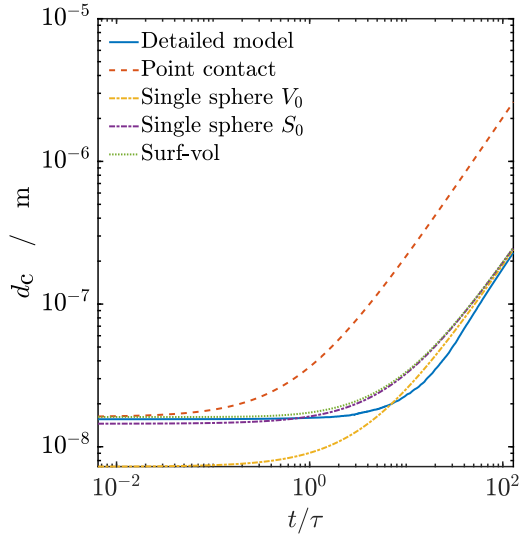

(c) Collision diameter

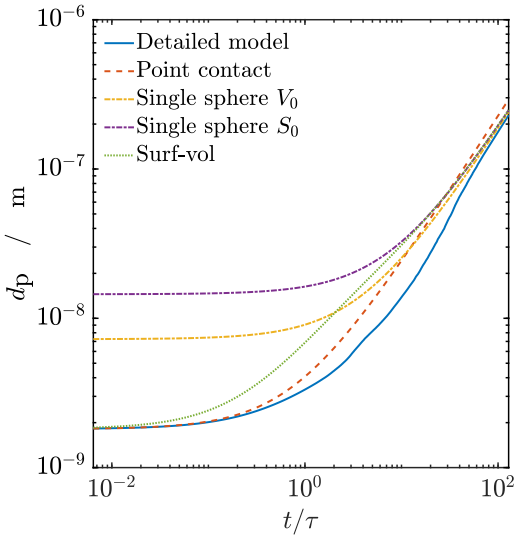

(d) Primary diameter

Figure S4: Evolution of particle properties as a function of dimensionless time for four different particle models undergoing collision limited growth. The single sphere cases with equivalent initial volume and surface area are distinguished by V_0 and S_0 respectively.

2.3. Surface area dependent growth

A growth rate proportional to the particle surface area is assumed:

$$\frac{\mathrm{d}V}{\mathrm{d}t} = \beta S. \tag{26}$$

2.3.1. Model equations

The detailed particle model is compared to the same three models as in the previous case of collision limited growth. The model equations are given below.

Primaries in point contact. For primary particles in point contact the primary radius evolves as

$$r_\mathrm{p} = r_{\mathrm{p},0} + \beta t. \tag{27}$$

Surface-volume model. The average primary radius and number of primaries are given by Eqs. (15) and (16). The model equations are

$$\frac{\mathrm{d}V}{\mathrm{d}t} = \beta S, \tag{28}$$

$$\frac{\mathrm{d}S}{\mathrm{d}t} = 4\beta\sqrt{\pi S}, . \tag{29}$$

These equations can be solved analytically:

$$V = \frac{1}{6\sqrt{\pi}}\left(2\sqrt{\pi}\beta t + 2\sqrt{\pi n_{\mathrm{p},0}}r_{\mathrm{p},0}\right)^3 + \frac{4}{3}\pi r_{\mathrm{p},0}^3\left(n_{\mathrm{p},0} - n_{\mathrm{p},0}^{3/2}\right), \tag{30}$$

$$S = \left(2\sqrt{\pi}\beta t + 2\sqrt{\pi n_{\mathrm{p},0}}r_{\mathrm{p},0}\right)^2. \tag{31}$$

Single sphere. The radius of single spherical particle evolves as

$$r = r_0 + \beta t, \tag{32}$$

where r_0 is the initial particle radius.

2.3.2. Results

The model test case was initialised with 64 primary particles of radius $r_{\mathrm{p},0} = 0.91$ nm in point contact. The point contact and surface-volume models assume a constant fractal dimension of $D_\mathrm{f} = 1.9$. In the case of the single sphere model, two different initial conditions were considered: equivalent initial mass

$$r_0 = r_{\mathrm{p},0}n_{\mathrm{p},0}^{1/3}, \tag{33}$$

and equivalent initial surface area

$$r_0 = r_{\mathrm{p},0}n_{\mathrm{p},0}^{1/2}. \tag{34}$$

For the new detailed particle model, 20 initial configurations were generated using the BCCA algorithm. Simulations were repeated twice.

Figure S5 shows the evolution of the (aggregate) particle volume, surface area, collision diameter and average primary diameter as a function of dimensionless time for the test case. The dimensionless time is defined as

$$\frac{t}{\tau} = \frac{\beta t}{r_{\mathrm{p},0}}. \tag{35}$$

Similar to the previous surface growth test case the point contact model displays significantly faster growth, while the detailed particle and surface-volume models converge on the spherical particle model at large t. The detailed particle model shows faster growth in particle volume and surface area than the surface-volume model and converges on the spherical model from above. This is a consequence of adding mass uniformly to the surface of the particle while maintaining a rigid structure. Meanwhile, the surface-volume model shows identical behaviour in surface area as a spherical particle with the same initial surface area, due to the rounding assumption. The collision diameters show very similar behaviour. The average primary diameter predicted by the detailed model diverges from the point contact model at $t = 10\tau$. The sudden nature of the divergence is due to the discrete treatment of coalescence events where two primaries are merged if they have sufficient overlap.

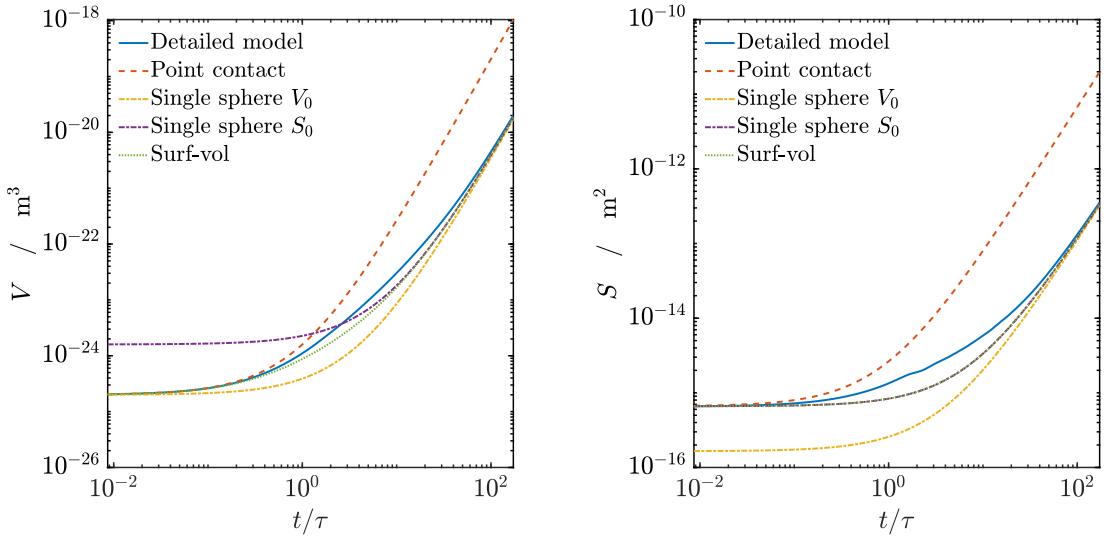

(a) Volume

(b) Surface area

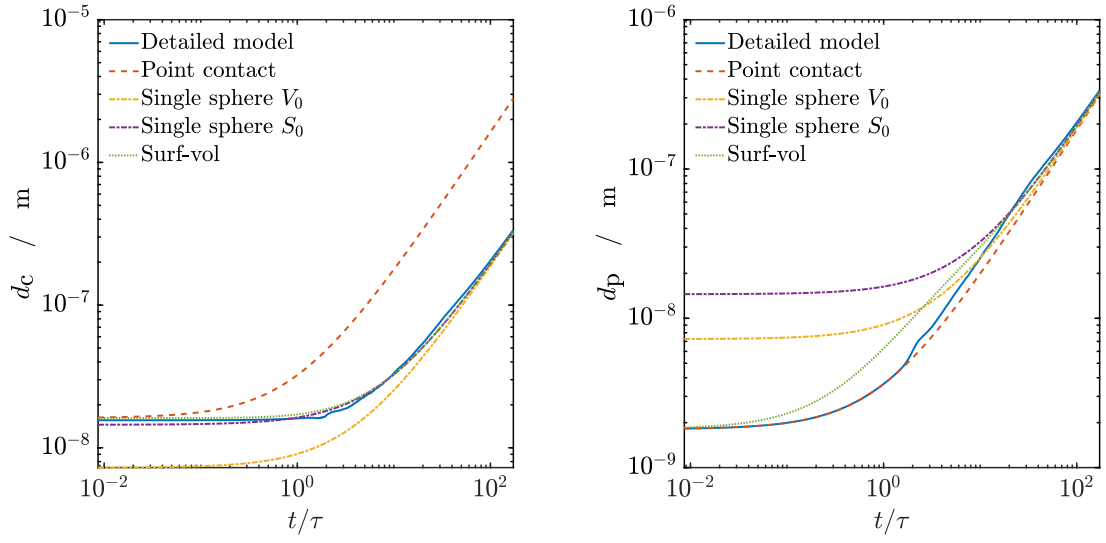

(c) Collision diameter

(d) Primary diameter

Figure S5: Evolution of particle properties as a function of dimensionless time for four different particle models undergoing surface area dependent growth. The single sphere cases with equivalent initial volume and surface area are distinguished by V_0 and S_0 respectively.

3. Sintering

The detailed particle model is compared to the commonly used model of Koch and Friedlander [5] (referred to as the "K-F model"):

$$\frac{\mathrm{d}S}{\mathrm{d}t} = -\frac{1}{\tau_\mathrm{s}}\left(S - S_\mathrm{f}\right), \tag{36}$$

where S is the surface area, S_f is the surface area of a sphere with same mass, and τ_s is the characteristic sintering time. The K-F model is implemented using a surface-volume particle description. Sintering is assumed to progress by grain boundary diffusion with characteristic sintering time

$$\tau_\mathrm{s} = \alpha r^4, \tag{37}$$

for a constant α. Two variations of this model are presented: sintering with constant $\tau_\mathrm{s} = \alpha r_0^4$, where the radius is taken as the initial primary radius, r_0; and sintering with variable $\tau_\mathrm{s} = \alpha r^4(t)$, where the primary radius evolves with time. In the latter case, the characteristic time is updated each time step. The model equations for the two cases are given below.

3.1. Model equations

3.1.1. Constant characteristic time

If the characteristic sintering time is kept constant, the surface area evolution is simply an exponential decay

$$S(t) = (S_0 - S_\mathrm{f}) \exp\left(-\frac{t}{\tau_\mathrm{s}}\right) + S_\mathrm{f}. \tag{38}$$

The initial surface area and volume are

$$S_0 = 4\pi r_0^2 n_\mathrm{p}, \tag{39}$$

$$V_0 = \frac{4}{3}\pi r_0^3 n_\mathrm{p}, \tag{40}$$

and the final surface area is the area of a single sphere with the same volume

$$S_\mathrm{f} = 4\pi\left(\frac{3V_0}{4\pi}\right)^{2/3}. \tag{41}$$

3.1.2. Variable characteristic time

If the characteristic time is allowed to vary with $r(t)$, Eq. (36) is expressed as

$$\frac{\mathrm{d}S}{\mathrm{d}t} = -\frac{S^4}{81\alpha V_0^4}\left(S - S_\mathrm{f}\right), \tag{42}$$

where we have used the relationship

$$r = \frac{3V_0}{S}, \tag{43}$$

to determine the primary radius [6]. Equation (42) is integrated numerically.

3.2. Results

The test case is initialised with 64 primary particles of radius $r_0 = 0.91$ nm in point contact. For the detailed particle model, 15 initial configurations were generated using the BCCA algorithm.

Figure S3 shows the evolution of the normalised surface area and average primary diameter against dimensionless time. To facilitate comparison of the models, a dimensionless time t^* is defined such that the excess surface has decreased by 63% at $t^* = 1$, i.e.

$$\frac{S(t^* = 1) - S_\mathrm{f}}{S_0 - S_\mathrm{f}} = e^{-1}. \tag{44}$$

This is consistent with the characteristic time of an exponential decay commonly used to model sintering.

The detailed particle model and K-F model with variable τ show similar sintering behaviour, particularly the evolution of the primary diameter. Over long times both cases are significantly slower than the constant τ model because their sintering rates vary as r^{-4}, which grows as the particles sinter.

The average primary diameter tends to the same value in all cases – that of a single sphere with the same initial volume. The average primary diameter predicted by the detailed model does not vary smoothly as the particle approaches a single sphere due to the imposed coalescence threshold, which merges two primaries once their level of sintering reaches 95% – introducing a step change in the diameter. This also causes the detailed model to approach the final primary diameter faster than the surface-volume model with variable τ. Otherwise, the two models are in very good agreement.

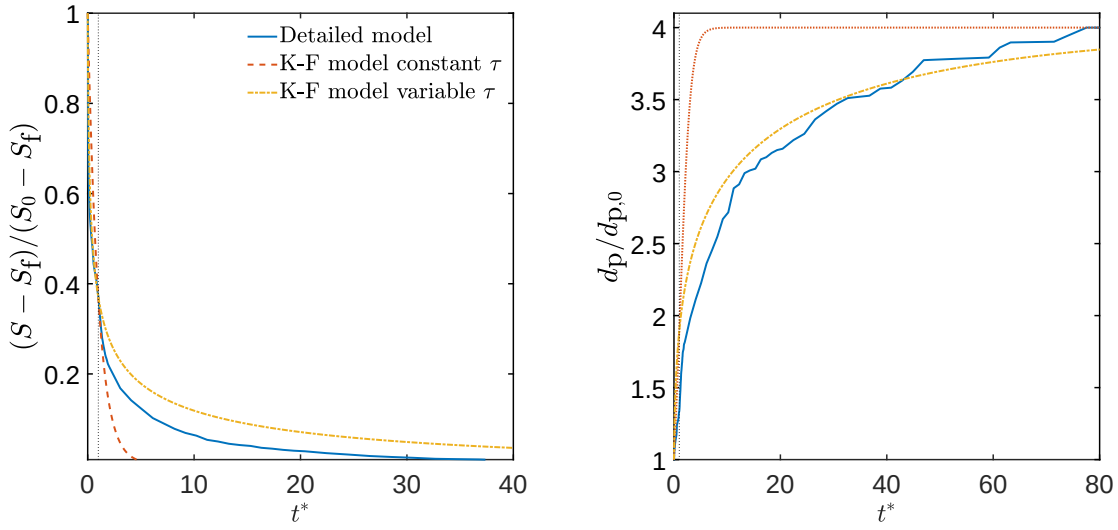

(a) Normalised surface area

(b) Normalised average primary diameter

Figure S6: Grain boundary sintering. The detailed particle model is compared to the model of Koch and Friedlander [5] with constant and variable characteristic time.

References

[1] R. Jullien, J. Phys. A: Math. Gen. 17 (1984) L771–L776.

[2] M. L. Eggersdorfer, S. E. Pratsinis, Aerosol Sci. Technol. 46 (2012) 347–353.

[3] T. Matsoukas, S. K. Friedlander, J. Colloid Interface Sci. 146 (1991) 495–506.

[4] R. I. A. Patterson, M. Kraft, Combust. Flame 151 (2007) 160–172.

[5] W. Koch, S. K. Friedlander, J. Colloid Interface Sci. 140 (1990) 419–427.

[6] F. E. Kruis, K. A. Kusters, S. E. Pratsinis, B. Scarlett, Aerosol Sci. Technol. 19 (1993) 514–526.